Supplementary material

Transferability of the SRP32-vdW specific reaction parameter functional to CHD_3 dissociation on Pt(110)-(2x1)

Helen Chadwick[1*†], Ana Gutiérrez-González[2], Rainer D. Beck[2] and Geert-Jan Kroes[1]

1. Leiden Institute of Chemistry, Gorlaeus Laboratories, Leiden University, P.O. Box 9502, 2300 RA Leiden, The Netherlands.

2. Laboratoire de Chimie Physique Moléculaire, Ecole Polytechnique Fédérale de Lausanne, CH-1015 Lausanne, Switzerland.

†. Current address. Department of Chemistry, Swansea University, Singleton Park, Swansea, SA2 8PP, United Kingdom.

***** Email address: h.j.chadwick@swansea.ac.uk

SI. Preparation of the Pt(110)-(2x1) Slab

The Pt(110)-(2x1) surface was modelled using a 9 layer (1x3) supercell, as shown schematically in Figure 1A of the main manuscript. A lattice parameter of 4.02 Å was used to generate the slab which has been determined using the SRP32-vdW functional previously[1], which is in reasonable agreement with the experimental value of 3.92 Å[2]. To obtain the optimized 0 K geometry of the slab, the top seven layers were allowed to relax in all three dimensions, with the bottom two layers fixed at their bulk positions. The changes in the interlayer distances d_{ij} and b_3, which are depicted in Figure S1, between the initial bulk structure and the relaxed structure are presented in Table SI alongside the values from previous experimental work and calculations. As discussed in the main manuscript, the relaxed interlayer distances are consistent with previous studies, but the value of b_3 is larger when the SRP32-vdW functional is used.

Twelve initial slabs were generated at a surface temperature of 650 K as in previous studies[1,3] by expanding the 0 K lattice parameters by 1.005[2] to account for the thermal expansion and randomly assigning initial displacements and velocities to the atoms in the top seven layers of the slab using the independent harmonic oscillators model. These slabs were then equilibrated for 1 ps, equilibrated with a thermostat for 1 ps, and then freely equilibrated for a further 2 ps. The initial conditions of the slab in the AIMD calculations were randomly sampled from the velocities and displacements obtained from all twelve slabs in the final 1 ps equilibration. These slabs had an average temperature of 658.8 K with a standard deviation of 77.2 K. The average interlayer distances for the equilibrated slabs, d_{ij} and b_3, are presented in Table SII. In addition, the angle between the facet and the Pt(110)-(2x1) plane, denoted θ_f in Figure S1, is also given.

SII. Convergence Tests

Convergence tests were run using the L2 transition state shown in Figure 10 of the main manuscript with the activation barrier, $E_b^{13\text{Å}}$, being determined as

$$E_b^{13\text{Å}} = \varepsilon_{TS}^{13\text{Å}} - \varepsilon_{\text{asym}}^{13\text{Å}} \quad \text{(S1)}$$

where $\varepsilon_{TS}^{13\text{Å}}$ is the absolute energy of the transition state, and $\varepsilon_{\text{asym}}^{13\text{Å}}$ the absolute energy of the molecule in its relaxed gas phase geometry positioned half-way between repeat periodic replicas of the slab (at 6.5 Å), both calculated with a 13 Å vacuum space. Calculations were run for slabs with different numbers of layers, different supercell sizes, different plane wave energy cut-offs and different sized Γ-centered K-point grids, with the activation barrier for the L2 transition state for each set-up presented in Table SIII. The top row shows the parameters used in the calculation, which has a chemically accurate barrier (its height being within 4.2 kJ/mol of the more converged calculations). The activation barriers for the L2, K1 and TS3 transition states from the set-up used in the AIMD calculations (in bold) are compared with the most converged values for each transition state in Table SIV. The barriers for the K1 and TS3 transition states in the AIMD calculations are also within chemical accuracy of the more converged barrier heights.

SIII. Residual Energy Correction

Figure S2 shows the potential energy curves calculated for the methane approaching the ridge (red), facet (blue) and valley (green) sites on the Pt(110)-(2x1) surface using a vacuum spacing of 13 Å (solid lines) and 30 Å (dashed lines), with Z representing the height of the center of mass of the molecule above the Pt(110)-(2x1) surface plane. The methane was held fixed in its relaxed gas phase geometry, with three H atoms pointing towards the surface. The energies calculated with 13 Å of vacuum spacing are larger because these calculations include interactions between periodic replicas of the slab due to the van-der Waals correlation

term in the SRP32-vdW functional. This interaction can be removed by increasing the vacuum spacing between the periodic replicas to 30 Å but this then makes the AIMD calculations too computationally expensive to run. As this interaction can be approximated by a constant increase in energy, the AIMD calculations were run, as previously[1,3,4], with the smaller vacuum spacing and with a small amount of additional translational energy added to the molecule to compensate for this energy shift. This residual energy, E_R, has been calculated using

$$E_R = E_{Z=6.5\text{Å}}^{13\text{Å}} - E_{Z=6.5\text{Å}}^{30\text{Å}} \quad \text{(S2)}$$

$E_{Z=6.5\text{Å}}^{13\text{Å}}$ and $E_{Z=6.5\text{Å}}^{30\text{Å}}$ are the energies relative to the asymptotic value when the molecule is 6.5 Å away from the surface in a cell with 13 Å and 30 Å vacuum spacing between periodic slab replicas, respectively. As shown in Figure S2, $E_{Z=6.5\text{Å}}^{13\text{Å}}$ = 0 kJ/mol and $E_R = -E_{Z=6.5\text{Å}}^{30\text{Å}}$. For the three different atoms in the surface, E_R is between 1.5 kJ/mol and 2.0 kJ/mol; we use the average value of 1.8 kJ/mol in the calculations. The effective activation barrier, E_b^e is then given by

$$E_b^e = E_b^{13\text{Å}} - E_R \quad \text{(S3)}$$

$E_b^{13\text{Å}}$ = 65.7 kJ/mol giving E_b^e = 63.9 kJ/mol which is within chemical accuracy of the activation barrier calculated with 30 Å of vacuum spacing, $E_b^{30\text{Å}}$, 62.3 kJ/mol validating our approach. All the values are given in Table SV.

SIV. Velocity Distributions and Sticking Coefficients

The stream velocity, v_0, and width parameter, α, of the velocity distributions obtained from time of flight measurements are given in Table SVI, alongside the nozzle temperature, T_N, and the corresponding average collision energy average energy, $\langle E_i \rangle$. The experimental and calculated sticking coefficients for each incident energy are presented in Table SVII.

Table SI A comparison of the differences between the bulk Pt(110)-(2x1) geometry and the relaxed Pt(110)-(2x1) geometry obtained in the present study (SRP32-vdW) and previous theoretical (NRL-TB[5], PW91[6], FLAPW[7], EAM[8] and MEAM[9]) and experimental (LEED[10,11] and MEIS[12]) studies.

	Δd_{12} (%)	Δd_{23} (%)	Δd_{34} (%)	b_3 (Å)
SRP32-vdW	-18.5	-0.2	1.1	0.35
NRL-TB[5]	-14.3	2.4	1.0	0.21
PW91[6]	-16	0.0	2.0	0.27
FLAPW[7]	-17.6	-0.5	N/A	0.25
EAM[8]	-17.6	-5.1	-0.7	0.11
MEAM[9]	-23.2	-2.6	N/A	0.29
LEED[10]	-17.4	1.1	0.4	0.17
LEED[11]	-18.4	-12.6	-8.7	0.32
MEIS[12]	-16 (3)	4 (3)	N/A	0.10

NRL-TB: Naval research laboratory tight binding method (Ref. 5)

PW91: Density functional theory with the PW91 functional (Ref. 6)

FLAPW: Full-potential linearized augmented plane wave method (Ref. 7)

EAM: Embedded atom method (Ref. 8)

MEAM: Modified embedded atom method (Ref. 9)

LEED: Low energy electron diffraction (Refs. 10 and 11)

MEIS: Medium energy ion scattering (Ref. 12)

TABLE SII The interlayer distances (d_{ij} and b_3) and angle between the facet and surface normal (θ_f) obtained using the SRP32-vdW functional for the relaxed 0 K slab geometry and averaged over the 650 K slab equilibration dynamics used to sample the initial conditions of the surface atoms in the AIMD calculations. The interlayer distances and angle are shown schematically in Figure S1.

	0 K	650 K
d_{12} (Å)	1.16	1.16 (0.03)
d_{23} (Å)	1.42	1.43 (0.01)
d_{34} (Å)	1.44	1.46 (0.01)
b_3 (Å)	0.35	0.37 (0.03)
θ_f (˚)	30.8	30.8 (0.2)

Table SIII The activation barriers, $E_b^{13\text{Å}}$, as a function of the number of layers of the slab, supercell size, plane wave energy cut-off (1 eV = 96.5 kJ/mol) and the size of the Γ-centered K-point grid. The final column shows the difference between the activation barrier and that from the set-up used in the AIMD calculations, shown in bold in the first row. All data is for the L2 transition state.

Layers	Supercell size	Energy cut-off (eV)	K-points	$E_b^{13\text{Å}}$ (kJ/mol)	$\Delta E_b^{13\text{Å}}$ (kJ/mol)
9	**1x3**	**400**	**3**	**65.7**	**0.0**
6	1x3	400	3	56.3	-9.3
7	1x3	400	3	70.5	4.9
8	1x3	400	3	58.2	-7.5
10	1x3	400	3	64.3	-1.3
11	1x3	400	3	60.9	-4.7
12	1x3	400	3	66.5	0.9
13	1x3	400	3	61.6	-4.1
14	1x3	400	3	63.4	-2.3
16	1x3	400	3	61.8	-3.9
18	1x3	400	3	63.2	-2.5
20	1x3	400	3	64.1	-1.6
22	1x3	400	3	63.4	-2.2
24	1x3	400	3	62.7	-3.0
9	1x2	400	3	67.7	2.0
9	2x2	400	3	66.7	1.0
9	2x3	400	3	65.1	-0.5
9	1x4	400	3	65.5	-0.2
9	2x4	400	3	64.7	-0.9
9	1x3	300	3	63.4	-2.3
9	1x3	350	3	65.3	-0.4
9	1x3	500	3	65.7	0.0
9	1x3	600	3	65.8	0.1
9	1x3	700	3	65.9	0.2
9	1x3	400	2	67.5	1.9
9	1x3	400	4	65.7	0.0
9	1x3	400	6	65.7	0.1
9	1x3	400	8	66.5	0.9
9	1x3	400	11	66.4	0.8

Table SIV The activation barriers, $E_b^{13\text{Å}}$, for the set-up used in the AIMD calculations (in bold) compared to those for the more converged set-ups for the L2, K1 and TS3 transition states.

Layers	Supercell size	Energy cut-off (eV)	K-points	$E_b^{13\text{Å}}$ (kJ/mol)	$\Delta E_b^{13\text{Å}}$ (kJ/mol)
L2					
9	**1x3**	**400**	**3**	**65.7**	**0.0**
22	1x3	400	3	63.4	-2.2
9	2x4	400	3	64.7	-0.9
9	1x3	400	11	66.4	0.8
K1					
9	**1x3**	**400**	**3**	**71.6**	**0.0**
22	1x3	400	3	69.5	-2.1
9	2x4	400	3	70.5	-1.2
9	1x3	400	11	72.0	0.4
TS3					
9	**1x3**	**400**	**3**	**96.5**	**0.0**
22	1x3	400	3	96.5	0.0
9	2x4	400	3	96.5	0.0
9	1x3	400	11	96.7	0.2

Table SV The activation barrier calculated using 30 Å ($E_b^{30\text{Å}}$) and 13 Å ($E_b^{13\text{Å}}$) vacuum spacing, the residual energy (E_R), the effective barrier (E_b^{e}) and the difference between $E_b^{30\text{Å}}$ and E_b^{e} determined using the SRP32-vdW functional for methane dissociation on Pt(110)-(2x1).

$E_b^{30\text{Å}}$ (kJ/mol)	62.3
$E_b^{13\text{Å}}$ (kJ/mol)	65.7
E_R (kJ/mol)	1.8
E_b^{e} (kJ/mol)	63.9
$E_b^{\text{e}} - E_b^{30\text{Å}}$ (kJ/mol)	1.6

Table SVI The average incident energy ($\langle E_i \rangle$), nozzle temperature (T_N), stream velocity (v_0) and width parameter (α) obtained from experimental time of flight distributions and used as inputs for the AIMD calculations.

$\langle E_i \rangle$ (kJ/mol)	T_N (K)	v_0 (m/s)	α (m/s)
57.5	298	2441	148
68.8	350	2670	164
79.3	400	2861	193
85.5	450	2968	212
95.4	500	3132	238
106.8	550	3309	272
118.8	600	3486	300
124.6	650	3571	302

Table SVII The average incident energy ($\langle E_i \rangle$), experimental sticking coefficient (S_0) and associated error (σ), calculated reaction probability excluding any contribution from trapped trajectories (p_i) and associated error (σ_i), calculated reaction probability assuming that all trapped trajectories react (p_i^T) and associated error (σ_i^T) and the total number of AIMD trajectories run for each incident energy (N_{tot}).

$\langle E_i \rangle$ (kJ/mol)	S_0	σ	p_i	σ_i	p_i^T	σ_i^T	N_{tot}
Laser-off							
57.5	0.010	0.005	-	-	-	-	-
68.8	0.021	0.005	-	-	-	-	-
79.3	0.030	0.005	-	-	-	-	-
85.5	0.041	0.005	-	-	-	-	-
95.4	0.059	0.006	0.031	0.005	0.078	0.008	1000
106.8	0.074	0.007	0.047	0.007	0.084	0.009	1000
118.8	0.092	0.009	0.062	0.008	0.078	0.008	1000
124.6	0.108	0.011	0.06	0.008	0.082	0.009	1000

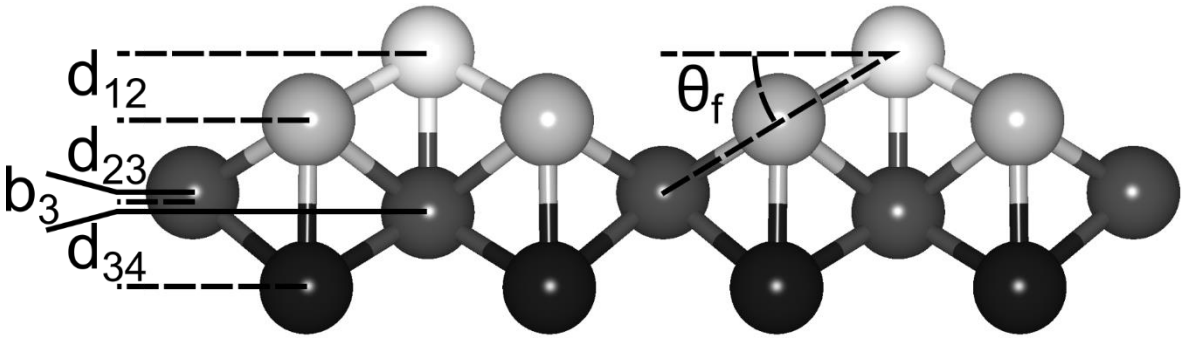

Figure S1 Schematic side view of the Pt(110)-(2x1) surface showing the interlayer distances d_{ij} and b_3 as well as the angle of the facet with respect to the plane of the Pt(110)-(2x1) surface, θ_f. The average height of the atoms in the third layer is used when determining d_{23} and d_{34}.

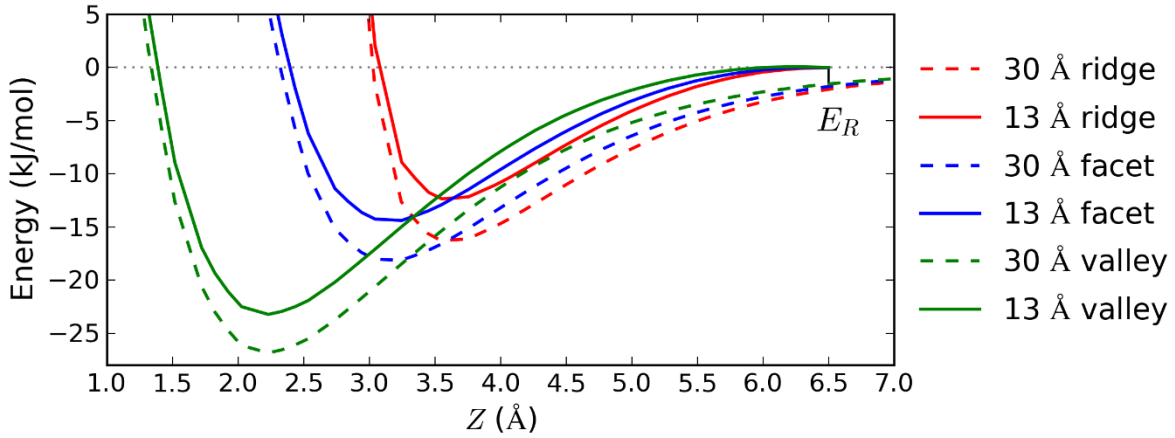

Figure S2 A comparison of the long range interactions calculated for methane above the ridge (red), facet (blue) and valley (green) atoms on Pt(110)-(2x1) using a 30 Å vacuum space (dashed lines) and 13 Å vacuum space (solid lines). The residual energy (E_R) is shown at 6.5 Å.

References

[1] D. Migliorini, H. Chadwick, F. Nattino, A. Gutiérrez-González, E. Dombrowski, E.A. High, H. Guo, A.L. Utz, B. Jackson, R.D. Beck, and G.J. Kroes, J. Phys. Chem. Lett. **8**, 4177 (2017).

[2] J.W. Arblaster, Platin. Met. Rev. **41**, 12 (2006).

[3] F. Nattino, D. Migliorini, G.J. Kroes, E. Dombrowski, E.A. High, D.R. Killelea, and A.L. Utz, J. Phys. Chem. Lett. **7**, 2402 (2016).

[4] H. Chadwick, A. Gutiérrez-González, D. Migliorini, R.D. Beck, and G.J. Kroes, J. Phys. Chem. C **122**, 19652 (2018).

[5] M.I. Haftel, N. Bernstein, M.J. Mehl, and D.A. Papaconstantopoulos, Phys. Rev. B **70**, 125419 (2004).

[6] S.J. Jenkins, M.A. Petersen, and D.A. King, Surf. Sci. **494**, 159 (2001).

[7] J.I. Lee, W. Mannstadt, and A.J. Freeman, Phys. Rev. B **59**, 1673 (1999).

[8] S.M. Foiles, Surf. Sci. **191**, L779 (1987).

[9] T. Yamaghishi, K. Takahashi, and T. Onzawa, Surf. Sci. **445**, 18 (2000).

[10] P. Fery, W. Moritz, and D. Wolf, Phys. Rev. B **38**, 7275 (1988).

[11] E.C. Sowa, M.A. Van Hove, and D.L. Adams, Surf. Sci. **199**, 174 (1988).

[12] P. Fenter and T. Gustafsson, Phys. Rev. B **38**, 10197 (1988).